

# THE GEOLOGICAL RECORD AS AN INDICATOR OF THE MUDSTONES THERMAL CHARACTERISTICS IN THE TEMPERATURE RANGE OF DECARBONATISATION

## GEOLOŠKI ZAPIS KOT POKAZATELJ TERMIČNIH LASTNOSTI LAPOROVCEV V TEMPERATURNEM OBMOČJU DEKARBONATIZACIJE

Željko Pogačnik<sup>1</sup>, Jernej Pavšič<sup>2</sup>, Anton Meden<sup>3</sup>

<sup>1</sup>Salonit Anhovo, Building Materials, Joint-Stock Co., Vojkova 1, 5210 Deskle, Slovenia

<sup>2</sup>Chair of paleontology and stratigraphy, University of Ljubljana, Privoz 11, 1000 Ljubljana, Slovenia

<sup>3</sup>Faculty of Chemistry and Chemical Technology, University of Ljubljana, Aškerčeva cesta 5, 1000 Ljubljana, Slovenia  
zeljko.pogacnik@salonit.si

Prejem rokopisa – received: 2008-10-03; sprejem za objavo – accepted for publication: 2008-12-06

The aim of this work is to find a connection between the marlstones geological record, i.e., its origin, and the thermal properties in the range of the decarbonatisation processes. As the geological record we took the recognized alteration or modification of the chemical and mineralogical difference, the amount of heavy metals and the fossilized nanoplankton material. For this research we collected and analyzed mudstones from four different lithological horizons of the subaqueous gravitational avalanche – turbidite, Paleocene flyschoidic rocks from the Anhovo area.

The remains of the nanoplankton fossilized skeletons are the main bearer of the amount of  $\text{CaCO}_3$  in this kind of sedimentary rock, besides a small quantity of carbonate fragments, mostly from older sedimentary rocks. We used optical microscopy, XRF, XRD and TGA-DTA analytical methods and granulometric analysis. The clay mineralogy was obtained from the acid residual XRD and DTG-DTA (temperature range to 1000 °C) analyses.

The research results demonstrated that we can expose four different groups of mudstones with similar thermal characteristics in the temperature range of the decarbonatisation. The chemical alternation degrees – the CIA of the rocks showed a connection between the clay mineralogy and the temperature course of the thermal decomposition of the mudstone carbonate. The quantity of nanoplankton skeletons followed a similar trend. The fundamental digressions in the heavy metals were not recognized, but the Ba quantity showed a good correlation with the samples that had a larger number of skeletons. We related this behavioural particularity with the biological activity of the environment. Both the CIA factor and the correlation of the skeleton number with the Ba content demonstrated different sedimentary environments and subsequently the influence of the geological record on the thermal decomposition nature of the rock in the range of decarbonatisation.

Key words: chemistry and mineralogy, cocolithophycae, mudstone thermal properties

V prispevku želimo poudariti povezavo med zgodovino (geološkega zapisa) nastanka laporovca litotipa mudstone in njegovimi termičnimi lastnostmi pri procesu dekarbonatizacije. Kot geološki zapis pojmujemo prepoznavno spremembo v kamnini, ki se kaže v njeni kemijski in mineraloški sestavi, vsebnosti težkih kovin in številu fosilnih skeletov kalcitnega nanoplanktona. V ta namen so bili analizirani vzorci laporovcev iz štirih litostatigrafskeh členov treh ciklotem (zaporedje kamnin, ki so nastale kot posledica delovanja podvodnih gravitacijskih plazov) paleocenske starosti na območju Anhovega.

Delež  $\text{CaCO}_3$  v laporovcih so večinoma skeleti mikrofossilov–kokolitoficej in karbonatni drobir. Vzorci so bili analizirani z optično mikroskopijo, XRF, XRD, TGA-DTA in granulometrijsko analizo. Za določitev mineralov glin so bili vzorci izpostavljeni kislinskemu razklpu s klorovodikovo kislino. Netopni ostanek je bil ponovno analiziran z XRD- in DTG-DTA-metodo v temperaturnem območju do 1000 °C.

Na osnovi rezultatov lahko med analiziranimi vzorci poudarimo štiri skupine, ki imajo podobne termične lastnosti v območju dekarbonatizacije. Stopnja kemijsko spremenjene kamnine-CIA kaže, da so količina mineralov glin in njihove spremembe povezane s temperaturnim potekom termičnega razpada laporovca tipa mudstone. Podobno usmeritev je opaziti tudi pri številu ohranjenih skeletov kokolitoficej. Bistvenih odmikov med vzorci glede vsebnosti težkih kovin ni opaziti, razlikujejo pa se v vsebnosti Ba, ki posredno z ohranjenimi skeleti kokolitoficej kaže na biološko aktivnost sedimentacijskega okolja. Tako faktor CIA kot število kokolitoficej kažeta različno sedimentacijsko okolje kamnine litotipa mudstone oz. da ima geološki zapis vpliv na lastnosti kamnine v temperaturnem območju dekarbonatizacije.

Ključne besede: kemizem in mineralogija, kokolitoficeje, termične lastnosti laporovcev

## 1 INTRODUCTION

The mineral raw material used to produce portland cement clinker (OPC) in the Anhovo area is bound to subaqueous gravitational avalanches<sup>1</sup>, which set off at unstable shores in the late Paleocene. The raw material consists of marly breccias, marly limestone and limestones, coarse-grained, medium-grained and fine-grained lime sandstones, marlaceous limestones and marls, and a

combination of shales, carbonate and silicyclastic siltstones and slatestones. The mudstones are carbonate sedimentary rocks with a silty base and a weight proportion of grains (either of organic or inorganic origin) not exceeding 10 %. The grains are 30 µm to 2 mm in diameter. They are typical of a calm and deep-water environment. In the pelagic environment the producers of carbonate material are mainly plankton organisms.

When a marly grain is thermally decomposed, a sharp edge is produced between a new CaO and a yet unreacted carbon core, showing that the grain decarbonatisation process is created first on the inside and then it spreads outside. The marls carry SiO<sub>2</sub>. Due to the genetic character of the rock, it is mostly equally spread and forms the basis as clay minerals in between carbonated particles. All the clay minerals lose bound water between the layers in the temperature range between 100 °C and 200 °C. First off, the minerals of the kaolinite groups fall apart between 450 °C (or 500 °C for the illite group) and 600 °C; they lose chemically bound OH in the process of complete decomposition. In the temperature range between 600 °C and 700 °C, the minerals of the montmorillonite group lose the OH group and this corresponds to the process area of decarbonatisation.

This article aims to emphasize the influence of the geological record of mudstone creation on its thermal characteristics in the process area of decarbonatisation, which is in the temperature interval between 650 °C and 950 °C. This adheres to the recognized rock change in the geological record, reflecting a direct or indirect sedimentary environment in which the rock has been created. The changes occur in the mineralogy and the preserved number of fossil remnants, indirectly indicating the biological and physico-chemical activities of the sedimentary environment.

## 2 MATERIAL SELECTION AND ANALYTICAL METHODS

The sampled minerals belong to the group of marly olistolithes of basal breccias (cyclothem Rodež and Perunk) and the marl of the upper cyclothem part Podbrdo. Due to the specific genesis<sup>3</sup> and rock position<sup>4</sup>

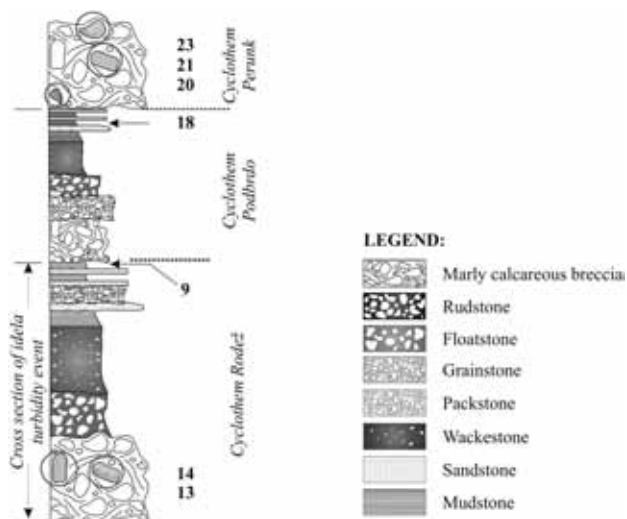


**Figure 1:** The classification of the analyzed samples in mega cycloths

**Slika 1:** Razporeditev analiziranih vzorcev v megaciklotemah

that involve the sites of mineral raw materials, significant differences between the individual eroded and pre-sedimented marls in flyschoidic cycloths need to be determined (**Figure 1**).

The following samples have been analyzed: Sample 13 and Sample 14 (eroded marlstones from marly calcareous breccia of cyclothem Rodež), marlstone Sample 9 (from the upper part of cyclothem Rodež), Sample 18 (marlstone of Podbrdo cyclothem), Sample 20, Sample 21 and Sample 23 (eroded marlstones from marly calcareous breccia of cyclothem Perunk). To determine the significant differences between the marlstones, the XRF and XRD analyses were carried out, along with the thermal methods (TG-DTG-DTA), the analysis of strong acid digestion, granulometric analysis of the insoluble residue and the petrographic microscopic analyses.

Part of the samples was crushed in a laboratory mill, and the rest was used to carry out the micro-paleontological analysis. We used a scraping tool to obtain some pulverized parts from the undamaged sample of the rock. Those parts were dissolved in the water, dried up and covered in Canadian balm. That preparation was then evenly distributed on the microscopic glass and covered with a square coverslip, the a side of 22 mm. We used transmitted light by applying cross nicols and regularly transmitted light magnified 1000 times; with a microscopic analysis we evaluated (per unit of surface area) the quantity of nanoplankton skeletons.

To determine the main oxides (SiO<sub>2</sub>, Al<sub>2</sub>O<sub>3</sub>, Fe<sub>2</sub>O<sub>3</sub>, CaO, MgO, K<sub>2</sub>O, Na<sub>2</sub>O, SO<sub>3</sub> and calculated CaCO<sub>3</sub> , assuming that the whole CaO is bound to carbonates) and certain metals (V, Ba, Ni, Cr, Ti in Mn), we used XRF analyses. The voltage and current of the x-ray tube of the ARL 8480 instrument were 30 kV and 80 mA, whereas the recording time was set to 40 s. The samples were examined by applying XRD analyses and the TG-DTG-TGA methods (defining CaCO<sub>3</sub> from the emitted CO<sub>2</sub>).

The samples for the XRD analysis were recorded on a PANalytical X'Pert PRO MPD diffractometer by applying the reflection technique and the CuK<sub>α1</sub> radiation in the 2θ range from 3° to 70° in steps of 0.034° 2θ, an integration time of 400 s, a 20-mm mask and a divergent and an antiscatter slit, set to 20 mm of the sample irradiation. Soller slits of 0.02 radians were used on both sides and the whole detector range was applied. The sample was rotated around the vertical axis. The Rietveld analysis of the diffraction pattern was performed with the TOPAS 3.0 programme and with the use of models containing 9 to 12 of the crystalline phases. In all cases a very good final match of the calculated and measured pattern with  $R_{wp}$  at around 6 % was obtained.

While analysing the samples with thermal methods, well-homogenized measured parts were heated in cylindrical pots (1 mm to 3 mm in height and 4 mm in diameter) made of inert materials (platinous and Al<sub>2</sub>O<sub>3</sub>

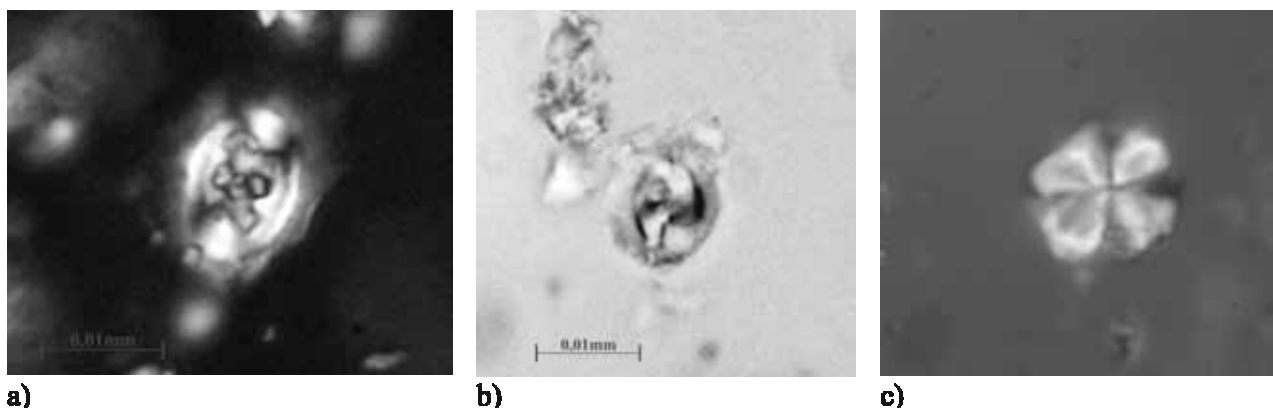


**Figure 2:** Calcite nanoplankton from the Sample 23: a) *Chiasmolithus bidens*, b) *Ellipsolithus macellus* in c) *Fasciculithus tympaniformis*. Pictures a) and c) are recorded under crossed nicols, b) is recorded by applying regular light.

**Slika 2:** Kalcitni nanoplankton iz vzorca 23: a) *Chiasmolithus bidens*, b) *Ellipsolithus macellus* in c) *Fasciculithus tympaniformis*. Sliki a) in c) sta posneti pod navzkrižnimi nikoli, b) pa pri navadni svetlobi.

pots) by applying a temperature scan of 10 °C/min at room temperature and up to 1400 °C. We used the STD 2960 Simultaneous DTA-TGA analyser to carry out this procedure. When the signal analysis was made, we elaborated on the temperature parameters, which are presented in **Table 1**, see below. The software tool *Universal Analysis for Windows 95/98/NT*, edition 2.5H, was used to define the parameters.

**Table 1:** Temperature parameters<sup>5,6,7</sup>

**Tabela 1:** Temperaturni parametri<sup>5,6,7</sup>

Parameter	Explanation
$T_2$	The temperature at which the reaction ends, corresponds to $T_{\text{offset}}$ (identified with 1. derivative of the TG-curve)
$T_{\text{onset}}$	The temperature which triggers the decomposition reaction – crystallization – is the lowest temperature which triggers the process $\neq T_1$
$T_{\text{max}}$	The temperature at which the process triggered reached its peak

To divide the clay component basis in marlstones, we carried out an acid decomposition of the samples. In a container with 450 mL of distilled water there was a 100-gram sample, to which we gradually added diluted hydrochloric acid (37 % concentrated HCl acid, mixed with distilled water in a 1:1 ratio) with a total capacity of 200 mL. The insoluble residue was decanted with distilled water to reach pH ≈ 4. Then the material was dried in a drier at 37 °C for 18 h. The samples obtained were passed through a sieve of 45 µm and the residue was analysed by applying the XRD-method and thermal analyses. On the basis of the results obtained, we evaluated the mineralogy of the insoluble residue.

### 3 RESULTS OF THE ANALYSIS

The microscopic analysis showed that Sample 23 (followed by Sample 21 and Sample 14 – **Table 2**) contains the largest number of fossil skeletons of the nanoplankton organisms.

**Table 2:** The number of fossil units (the number on the diameter area of 22 mm<sup>2</sup>) in the individual sample

**Tabela 2:** Število fosilnih enot (št. na površini premera 22 mm<sup>2</sup>) v posameznem vzorcu

SAMPLE	Number of units
Sample 9	162
Sample 13	142
Sample 14	370
Sample 18	120
Sample 20	165
Sample 21	468
Sample 23	880

In Sample 23, besides many other types of calcite nanoplankton, we also detected the following types (**Figure 2**): *Chiasmolithus bidens* (Bramlette et Sullivan), *Ellipsolithus macellus* (Bramlette et Sullivan) ter *Fasciculithus tympaniformis* (Hay et Mohler).

According to the proportion of the calcium carbonate, determined on the basis of the emitted CO<sub>2</sub> at the decarbonatisation process (**Table 3**), we concluded that

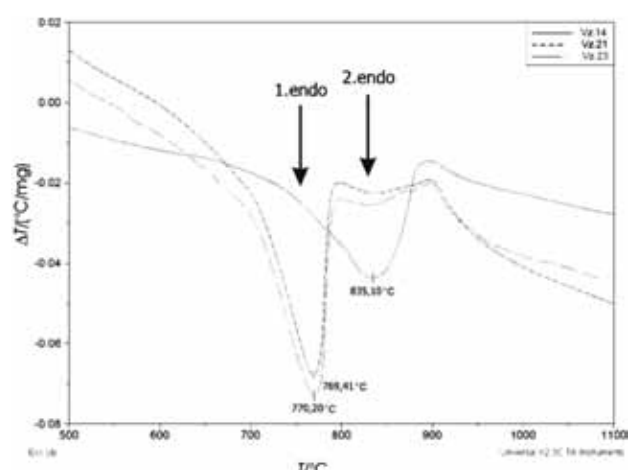


**Figure 3:** DTA curves of the Samples 21, Sample 23 and Sample 14  
**Slika 3:** DTA krivulja vzorcev Vz. 21, Vz. 23 in Vz. 14

**Table 3:** The results of the XRF- and TG-DTG-DTA analyses of the primary sample  
**Tabela 3:** Rezultati XRF- in TG-DTG-DTA analize osnovnega vzorca

SAMPLE	proportion CO <sub>2</sub>	CaCO <sub>3</sub> <sup>to</sup>	Ti	SiO <sub>2</sub>	Al <sub>2</sub> O <sub>3</sub>	Fe <sub>2</sub> O <sub>3</sub>	CaO	MgO	K <sub>2</sub> O	Na <sub>2</sub> O	CaCO <sub>3</sub>	V	Ba	Ni	Cr	Mn
	TG-DTG-DTA		XRF													
	(mass proportion, w/%)														w/(µg/g)	
Smp. 9	23.65	53.75	0.15	19.60	5.16	2.40	37.65	1.37	1.11	0.22	67.21	56	550	53	54	568
Smp. 13	25.29	57.48	0.14	18.96	4.73	2.28	38.18	1.49	1.02	0.21	68.16	49	454	52	53	499
Smp. 14	26.73	60.75	0.16	21.80	5.52	2.80	35.33	1.67	1.25	0.25	63.07	61	457	60	57	533
Smp. 18	25.75	58.52	0.15	20.74	4.83	2.25	37.48	1.40	1.00	0.26	66.90	54	324	50	57	381
Smp. 20	23.70	53.86	0.15	21.05	4.85	2.28	37.34	1.38	1.00	0.26	66.65	52	377	51	58	382
Smp. 21	19.14	43.50	0.20	26.14	6.71	3.09	32.39	1.42	1.32	0.18	57.81	66	199	65	66	463

**Table 4:** TG-DTG-DTA analysis of the original sample and the insoluble residue (the residue on a sieve of 45 µm) in the temperature interval of decarbonatisation

**Tabela 4:** TG-DTG-DTA-analiza originalnega vzorca in netopnega ostanka (ostanek na situ 45 µm) v temperaturnem intervalu dekarbonizacije

SAMPLE	Analysis of the original sample					
	T <sub>onset</sub>	T <sub>max</sub>	T <sub>max</sub> -T <sub>onset</sub>	T <sub>2</sub>	CO <sub>2</sub>	CaCO <sub>3</sub>
	°C			w/%		
Smp. 9	717.13	778.62	61.49	812.60	23.65	53.75
Smp. 13	715.62	779.58	63.96	812.70	25.29	57.48
Smp. 14	757.94	835.10	77.16	911.00	26.73	60.75
Smp. 18	716.18	786.78	70.60	825.30	25.75	58.52
Smp. 20	713.88	777.31	63.43	809.50	23.70	53.86
Smp. 21	709.51	769.41	59.90	798.40	19.14	43.50
Smp. 23	706.43	770.20	63.77	801.60	18.68	42.45
Analysis of the insoluble sample residue on the sieve of 45 µm						
Smp. 9	-	-	-	-	-	-
Smp. 13	682.91	767.27	84.36	798.90	23.13	52.57
Smp. 14	728.26	795.22	66.96	824.90	10.61	24.11
Smp. 18	695.72	777.98	82.26	809.76	27.47	65.18
Smp. 20	682.91	767.27	84.36	798.90	23.13	62.43
Smp. 21	-	-	-	-	-	-
Smp. 23	636.58	751.11	114.53	837.60	10.52	23.91

Sample 14 contains the largest amount of carbonate, whereas Sample 21 and Sample 23 contain the smallest amount.

**Figure 3** shows concave curves of the DTA samples 23, 21 and 14. The number of DTA signals shows at least two endothermic reactions in the range of the thermal decomposition of carbonate, whereas the curve of Sample 14 has an extremely low amplitude and a shifted T<sub>max</sub>.

The TG-DTG-DTA analysis of the insoluble residue in the decarbonatisation range shows strong endothermic peaks; they show characteristic temperatures at the beginning of the reaction and maximum temperatures at the very end of the reaction of the thermal carbonate decomposition (see **Table 4**).

The results of the XRD analysis (**Table 5**) show the presence of carbonate in the insoluble residue.

In all the primary samples the calcite is dominant, and flexures of different clay minerals at low angles can be clearly seen. Besides calcite, the following were also defined in the primary sample: quartz (SiO<sub>2</sub>), muscovite (KAl<sub>2</sub>(AlSi<sub>3</sub>O<sub>10</sub>)(OH)<sub>2</sub>), vermiculite (Mg<sub>4</sub>(AlSi<sub>3</sub>O<sub>10</sub>)(OH)<sub>2</sub>(H<sub>2</sub>O)<sub>4</sub>), kaolinite (Al<sub>2</sub>(Si<sub>2</sub>O<sub>5</sub>)(OH)<sub>4</sub>), kronstedtite (Fe<sub>3</sub>(FeSi)<sub>5</sub>(OH)<sub>4</sub>), cristobalite (SiO<sub>2</sub>), illite (K(Al<sub>4</sub>Si<sub>2</sub>O<sub>9</sub>(OH)<sub>3</sub>)), dolomite (CaMg(CO<sub>3</sub>)<sub>2</sub>), ankerite (CaFe(CO<sub>3</sub>)<sub>2</sub>), aragonite CaCO<sub>3</sub> and protoenstatite (MgSiO<sub>3</sub>). In the insoluble residue the calcite was not identified in samples 9 and 21. The proportion of false analysis is 3 % absolute with calcite, 1 % with muscovite, kaolinite and illite and 0.5 % with other components. Total proportion of the unidentified crystalline

**Table 5:** XRD and TG-DTG-DTA determination of certain mass proportions of minerals (%) in the primary sample (BULK) and its insoluble residue (<45 µm)

**Tabela 5:** XRD-in TG-DTG-DTA-določitev nekaterih masnih deležev mineralov (%) v osnovnem vzorcu (BULK) in njegovem netopnem ostanku (<45 µm)

SAMPLE	Kaolinite Al <sub>2</sub> (Si <sub>2</sub> O <sub>5</sub> )(OH) <sub>4</sub>		Illite K(Al <sub>4</sub> Si <sub>2</sub> O <sub>9</sub> )(OH) <sub>3</sub>		Muscovite KAl <sub>2</sub> (AlSi <sub>3</sub> O <sub>10</sub> )(OH) <sub>2</sub>		Illite/ muscovite	Albite NaAlSi <sub>3</sub> O <sub>8</sub>	Calcite CaCO <sub>3</sub>	Calcite CaCO <sub>3</sub>
	BULK	45 µm<	BULK	BULK	BULK	<45 µm				
Smp. 9	3.30	9.32	3.81	9.26	35.38	8.84	75.53	-		
Smp. 13	2.97	2.87	3.94	9.04	13.63	7.25	73.13	57.84		
Smp. 14	3.04	5.72	4.91	9.46	36.31	7.96	72.73	14.46		
Smp. 18	2.52	1.03	3.58	9.06	8.78	4.49	74.60	74.75		
Smp. 20	2.69	2.04	3.70	9.05	10.19	4.38	74.07	71.22		
Smp. 21	2.81	7.13	5.47	11.23	45.67	8.02	69.71	-		
Smp. 23	2.81	5.52	6.20	8.84	35.97	5.72	71.06	23.84		

phases is evaluated to less than 5 %; the amorphous phase is probably less than 10 %.

#### 4 DISCUSSION

The number of determined nanoplankton skeletons (**Table 1**) can be compared to the determined carbonate proportion in the individual sample (**Tables 2 and 3**). The difference can occur because of the group of carbonate minerals, parts of them, not bound to the then existing living environment of the nanoplankton organisms.

This is confirmed by the results of the diffraction and thermal analyses. The data show that the samples differentiate by the process type of decarbonatisation (double endothermic peaks; **Figure 3**), in the  $T_{\text{onset}}$  temperature and in the time to reach the maximum temperature of the carbonate decomposition ( $T_{\text{max}}$ , **Table 4**). In the sifted residue of the acid-treated sample (the size of grains below 45 µm) there is an unreacted carbonate (TG-DTG and XRD analyses), showing the presence of relatively older carbonate rocks that were eroded off from the older beds in the sedimentation process (of subaqueous avalanche) or brought in from the different sedimentary environment (most likely diagenetically already altered – aluminosilicate cement).

The interdependence of the mudstone rock samples from the Paleocene flyschoidic beds on the level of the temperature parameters ( $T_{\text{onset}}$ ,  $T_{\text{max}}$  in  $T_{\text{max}}-T_{\text{onset}}$ ), the geological record indicating when the marlstones were created (*CIA*<sup>\*</sup>,  $\text{K}_2\text{O}/\text{Al}_2\text{O}_3$ ,  $\text{K}_2\text{O}+\text{Na}_2\text{O}$ ,  $\text{K}_2\text{O}$ ,  $\text{CaCO}_3$ ,  $\text{Cr}/\text{Ni}$ ,  $\text{Cr}/\text{V}$ ,  $\text{Mn}$ ,  $\text{Ti}/\text{Al}$ ,  $\text{K}/(\text{Fe}+\text{Mg})$ ,  $\text{Ba}$  and the number of skeletons) and the ratio  $F^{**}$  are summarized in the **Table 6**.

Through a statistical overview of the results it can be concluded that the *CIA* factor and the number of preserved cocolithophyceae skeletons have a great influence on the start-up reaction temperature  $T_{\text{onset}}$  and the maximum temperature of the reaction process  $T_{\text{max}}$ . From the geological record it can also be concluded that K-aluminosilicates and clay minerals are prevalent in the samples (as shown by the results of the diffraction analysis – **Table 5**). The influence is shown in the  $T_{\text{max}}-T_{\text{onset}}$  temperature interval. Diagenesis runs were made to disintegrate the acid feldspars (orthoclase) into K-feldspars and further into clay minerals. In our case, the diffraction analysis did not identify the orthoclase; the albite, however, was identified. It appears together like the mineral joint with orthoclase in medium and acid magmatic rocks.

**Table 6:** Correlation table of the temperature parameters, the geological record of the marlstones and the F ratio  
**Tabela 6:** Korelacijska tabela temperaturnih parametrov, geološkega zapisa laporovcev in razmerja F

	<i>F</i>	$T_{\text{onset}}$	$T_{\text{max}}$	$T_{\text{max}}-T_{\text{onset}}$	<i>CIA</i>	$w(\text{K}_2\text{O})/w(\text{Al}_2\text{O}_3)$	$w(\text{K}_2\text{O} + \text{Na}_2\text{O})$	$w(\text{CaCO}_3)$	št. skeletov	$w(\text{Ba})$	$w(\text{K}_2\text{O})$	$w(\text{Cr})/w(\text{V})$	$w(\text{Cr})/w(\text{Ni})$	$w(\text{K})/w(\text{Fe} + \text{Mg})$	$w(\text{Ti})/w(\text{Al})$	$w(\text{SiO}_2)/w(\text{Al}_2\text{O}_3)$
<i>F</i>	1															
$T_{\text{onset}}$	0.892	1														
$T_{\text{max}}$	0.932	0.990	1													
$T_{\text{max}}-T_{\text{onset}}$	0.946	0.853	0.917	1												
<i>CIA</i>	0.770	0.871	0.898	0.876	1											
$w(\text{K}_2\text{O})/w(\text{Al}_2\text{O}_3)$	0.836	0.828	0.803	0.644	0.507	1										
$w(\text{K}_2\text{O} + \text{Na}_2\text{O})$	0.617	0.433	0.509	0.669	0.336	0.317	1									
$w(\text{CaCO}_3)$	0.859	0.648	0.676	0.682	0.341	0.867	0.616	1								
The No. of skeletons	0.765	0.919	0.879	0.665	0.731	0.895	0.149	0.592	1							
$w(\text{Ba})$	0.479	0.461	0.416	0.238	0.054	0.846	0.131	0.710	0.675	1						
$w(\text{K}_2\text{O})$	-0.289	0.009	-0.011	-0.066	0.377	-0.402	-0.469	-0.719	0.042	-0.518	1					
$w(\text{Cr})/w(\text{V})$	-0.385	-0.653	-0.596	-0.367	-0.570	-0.505	-0.029	-0.178	-0.718	-0.331	-0.315	1				
$w(\text{Cr})/w(\text{Ni})$	-0.075	-0.366	-0.312	-0.122	-0.524	-0.188	0.584	0.271	-0.553	-0.060	-0.763	0.558	1			
$w(\text{K})/w(\text{Fe} + \text{Mg})$	-0.582	-0.266	-0.317	-0.429	-0.056	-0.471	-0.514	-0.780	-0.117	-0.310	0.795	-0.400	-0.546	1		
$w(\text{Ti})/w(\text{Al})$	0.073	-0.192	-0.143	0.014	-0.349	-0.095	0.623	0.352	-0.444	-0.123	-0.748	0.449	0.948	-0.646	1	
$w(\text{SiO}_2)/w(\text{Al}_2\text{O}_3)$	0.269	-0.029	0.041	0.238	-0.157	0.029	0.735	0.474	-0.303	-0.054	-0.729	0.550	0.885	-0.791	0.925	1

\*  $\text{CIA} = \frac{w(\text{Al}_2\text{O}_3)}{w(\text{Al}_2\text{O}_3) + w(\text{CaO}) + w(\text{Na}_2\text{O}) + w(\text{K}_2\text{O})} \cdot 100$ ; proportion of  $\text{CaO}^+$  is a calculated proportion of CaO on the basis of the CaO difference, set by XRF-analysis and CaO, defined with the decarbonatisation process applying DTG-DTA-analysis.

\*\*  $F = \frac{w(\text{CaO}_t)}{w(\text{CaO}_f)}$ ,  $\text{CaO}_t$  is a calcium oxide, which is created through decarbonatisation process and the proportion of  $\text{CaO}_t$  is bound to an absolute quantity of Ca-oxide, defined in the sample on the basis of XRF-analysis.

The proportion of heavy metals in the samples (**Table 3**) is shown by the influence of the disintegrated ultramafic complex<sup>9</sup> (correlation between Cr/Ni and Cr/V with  $\text{SiO}_2/\text{Al}_2\text{O}_3$  proportion, **Table 6**) and the terigen insertion of individual minerals in the source of the clay component in the marlstones. Titanium is an extremely conservative trace element<sup>10</sup> and as such it is resistant to diagenetic factors, while the Al proportion has a dominant role in indicating the clay minerals. The correlation between Ti/Al and  $\text{SiO}_2/\text{Al}_2\text{O}_3$  (**Table 6**) shows that Ti entered the sedimentary environment through the river input or through earlier, eroded sedimentary rocks.

The hypothesis about the vulcanoclastic source of sediments is not acceptable, as this theory is disproved by a negative correlation<sup>10</sup> between the Ti/Al and the K/(Fe+Mg). The proportion of Mn<sup>11</sup> in the samples also shows the terigen import of the sediment or presedimentation. The negative correlation between the Ba and K<sub>2</sub>O shows that Ba is not bound to the clay component<sup>12</sup>, although Ba<sup>2+</sup> and K<sup>+</sup> can interchange in the crystal structure. So the source of Ba is to be ascribed to a general carbonate cycle, which corresponds to the ratio of CaCO<sub>3</sub> proportion and the number of nanoplankton skeletons in individual samples (**Table 2**).

## 5 CONCLUSION

The thermal analysis results show that marlstones of the mudstone lithotype react differently during the decarbonatization process (**Figure 4**) in the temperature range between 650 °C and 950 °C. Four groups can be distinguished among the curves. The two pairs of curves of the Sample 23 and Sample 21 are prominent among them, having two endothermic peaks. Sample 18 and Sample 13 are also worth mentioning, with the second endothermic peak being less emphasized.

The oldest marlstones – olistolithes (Sample 13 and Sample 14) – taken from a marly calcareous breccia

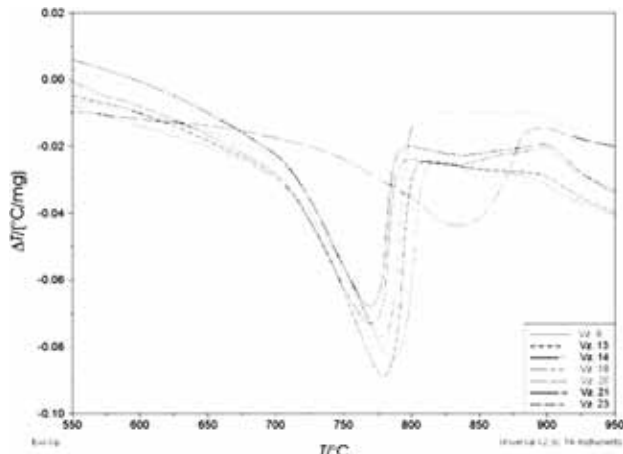


**Figure 4:** Comparison of marlstone DTA curves of mudstone type  
**Slika 4:** Primerjava DTA-krivulj laporovcev tipa mudstone

comper with Sample 9, from the upper part of the Rodež cyclothem, have the highest *F* ratio among all the samples, considering their lithostratigraphic sequence. They differ from one another in the number of nanoplankton skeletons and in the proportion of chemical change CIA factor. We can therefore conclude that the rocks were formed in two different sedimentary environments.

The marlstones of the Podbrdo cyclothem (Sample 18) differ from the previously mentioned samples in the quantity of the biogenic carbonate (number of skeletons) and Ba proportion, therefore confirming the biological activity of the environment. They also differ in the CIA factor, which is lower in the sample richer in fossils. In Sample 18 carbonate was identified in the insoluble residue; we therefore assume that in the sedimentation period different sources of carbonate material were present.

The marlstone samples (Sample 21, Sample 23 and Sample 20), taken in the youngest horizon of the marly calcareous breccia of Perunk cyclothem, differ from one another by the *F* ratio. Among the marlstones of this lithological horizon the *F* value is larger in the samples which hold a higher proportion of Ba. The number of skeletons and the content of Ba show that there are at least two different sedimentary environments to be distinguished in this marlstone group.

The CIA proportion (**Figure 5**) confirms that the number of feldspars and clay minerals, and the accordingly bound diagenetic changes, are related to the temperature process of the thermal decomposition of the carbonate rock. This is also evident from the correlation factor between the CIA and the start-up reaction temperature  $T_{\text{onset}}$ , as well as the maximum decarbonatization temperature  $T_{\text{max}}$ . A similar trend can be seen in the number of preserved coccolithophycae skeletons. Despite

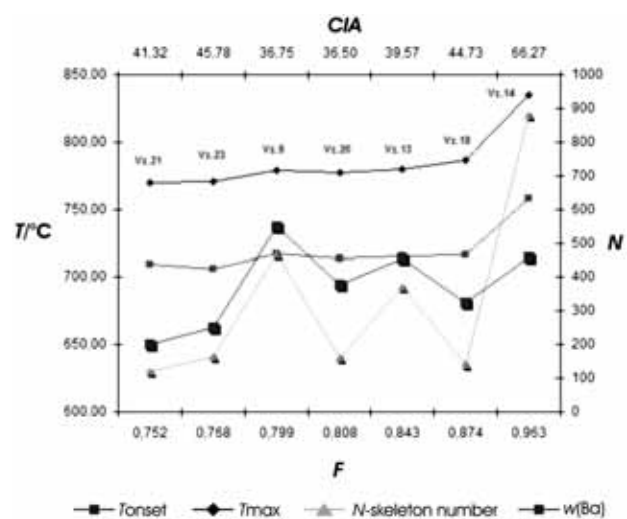


**Figure 5:** The ratio between the number of skeletons, Ba proportion ( $\mu\text{g/g}$ ), start-up reaction temperature  $T_{\text{onset}}$  (°C) and the *F* factor  
**Slika 5:** Razmerje med številom skeletov, deležem Ba ( $\mu\text{g/g}$ ), temperaturom začetka reakcije  $T_{\text{onset}}$  (°C) in faktorjem *F*

the approximately even number of skeletons the curves of Sample 23 and Sample 13 are shaped differently. The difference can be seen in the *CIA* ratio, as the latter is 13 % higher in Sample 23 than in Sample 13.

The proportion of heavy metals indicates the source of fine-grained material<sup>13</sup> (most likely the area of today's Carnic Alps), whereas the number of preserved skeletons and the Ba content indicate the change of the sedimentary environment in which the rock was created. The proportion of carbonate in the insoluble residue still remains unknown at this stage, although it does allow for the hypothesis of the material in the sample being of secondary origin (either presedimented or eroded from older cyclothem).

The highest CaO proportion, bound in carbonate, and the largest amount of cocolithophyceae can be found in Sample 14. This is followed by Sample 18, having the largest carbonate proportion in the insoluble residue; here the ratio between Ba and the number of skeletons allows for the hypothesis of the larger carbonate proportion being bound to fossil pelagic organisms, i.e. it is of biogenic origin.

The marlstone reflects the chemical and mineralogic features influencing the temperature reaction process in the carbonate decomposition range. The results of the analysis show that a sole definition of the rock lithotype does not clearly establish the temperature characteristic of the sedimentary rock <sup>2</sup> in the decarbonatisation area. Consequently, the geological record has an important influence on the temperature range of the decarbonatisation of the mudstone rock in the Paleocene sedimentary environment in the close-by area of Anhovo.

## 6 REFERENCES

- <sup>1</sup> Skaberne, D. Sedimentological investigation of flysch from the Anhovo area. Diploma degree (in Slovene), Katedra za geologijo in paleontologijo, NTF, Ljubljana, 1973, 285
- <sup>2</sup> Dunham, R. J. Classifications of carbonate rocks according to depositional texture. V: Clasification of Carbonate Rocks, a Symposium. Edited by Ham, E.W. Tulsa, (1962), 108–122
- <sup>3</sup> Skaberne, D. Observation Point N° II/9, The Paleocene megaturbides – Anhovo. V Evolution of the karstic carbonate platform – Excursions Guidebook, 5. June – 6. June. Trieste : Università degli studi di Trieste, Instituto di geologia e paleontologia, 1987, 37–45
- <sup>4</sup> Pogačnik, Ž., Car, M. Prostorska umestitev fliša v okolici Rodež-integrirani raziskovalni pristop. In: Horvat, Aleksander (ur.). 18. posvetovanje slovenskih geologov, (Geološki zbornik, 19). Ljubljana: Univerza v Ljubljani, Naravoslovno-tehniška fakulteta, Oddelek za geologijo, 2007, 92–96
- <sup>5</sup> Mackenzie, R. C. The differential thermal investigation of clays. London: Mineralogical society (clay minerals group), 1957, 456 str.
- <sup>6</sup> Ramachandran, V. S., Phil, D. Applications of differential thermal analysis in cement chemistry. Chemical publishing company, 1969, 308
- <sup>7</sup> Yen, F. S., Lo, H. S., Wen, H. L., Yang, R. J.  $\theta$  – to  $\alpha$  – phase transformation subsystem induced by  $\alpha$  –  $Al_2O_3$  – seeding in boehmite – derived nano – sized alumina powders. Journal of Crystal Growth, (2003), 249, 283–293
- <sup>8</sup> Nesbitt, H. W., Young, G. M. Early Proterozoic climates and plate motions inferred from major element chemistry of lutites. Nature, (1982) 299, 715–717
- <sup>9</sup> Barbara B., McLennan, S. M., Hanson, G. N. Geochemistry and provenance of the Middle Ordovician Austin Glen Member (Normanskill Formation) and the Taconian Orogeny in New England. Sedimentology 45 (1998), 635–655
- <sup>10</sup> Meyers, S. R., Sageman, B. B., Hinnov, L. A. Integrated quantitative stratigraphy of the Cenomanian–Turonian Bridge Creek limestone member using evolutive harmonic analysis and stratigraphic modeling. Journal of Sedimentary Research, 71 (2001), 4, 628–644
- <sup>11</sup> Veizer, J., Demovič, R. Environmental and climatic controlled fractionation of elements in the mesozoic carbonate sequences of the western Carpathians. 1. Journal of Sedimentary Research, 43 (1973) 1, 258–271
- <sup>12</sup> Dinelli, E., Lucchini, F., Mordini, A., Paganelli, L. Geochemistry of Oligocene-Miocene sandstones of the northern Apennines (Italy) and evolution of chemical features in relations to provenance changes. Sedimentary Geology, 127 (1999), 193–207
- <sup>13</sup> Venturini, S., Tunis, G. La composizione dei conglomerati cenozoici del Friuli: dati preliminari. In: Studi Geologici Camereti, Studi preliminari all'acquisizione dati del profilo CROP 1-1A La Spezia-Alpi orientali, 1992, 285–295